World Journal of Advanced Research and Reviews
eISSN: 2581-9615 CODEN (USA): WJARAI
Cross Ref DOI: 10.30574/wjarr
Journal homepage: https://wjarr.com/

(RESEARCH ARTICLE)

Check for updates

Influence of incorporating annealed fiber scraps on the physico-mechanical properties of ordinary concrete

Seick Omar SORE [1, 2], Philbert NSHIMIYIMANA [2, *], Abdel Aziz TINTO [1], P. Romel Gontran YERBANGA[1], Patrice SAWADOGO [3] and Adamah MESSAN [2]

[1] *Département Génie Civil de l'Institut Universitaire de Technologie / Laboratoire de Chimie et Energies Renouvelables (LaCER), Unité de Recherche en Physico-Chimie et Technologie des Matériaux, Université Nazi BONI, B.P. 1091 Bobo 01, Burkina Faso.*
[2] *Laboratoire Eco-Matériaux et Habitats Durables (LEMHaD), Institut International d'Ingénierie de l'Eau et de l'Environnement (Institut 2iE), 1 Rue de la Science, 01 BP 594 Ouagadougou 01, Burkina Faso.*
[3] *Laboratoire National du Bâtiment et des Travaux Publics (LNBTP), Direction régionale de Bobo-Dioulasso, 01 B.P. 3046 Bobo-Dioulasso 01, Burkina Faso.*

World Journal of Advanced Research and Reviews, 2025, 28(03), 974-987

Publication history: Received 23 October 2025; revised on 30 November 2025; accepted on 15 December 2025

Article DOI: https://doi.org/10.30574/wjarr.2025.28.3.4040

Abstract

Concrete is generally reinforced with steel bars tied together with annealed fibers, a process that generates metal fiber scraps, a form of construction waste. The presence of these residues around the construction site is a subject of debate among professionals; some see them as potential reinforcement of concrete, whereas others consider them as waste. This study aimed to evaluate the influence of adding annealed fiber scraps on the physical and mechanical properties of ordinary concrete. Composites were designed with fiber contents ranging from 0 to 0.75% of the concrete volume. Tests were carried out on cylindrical specimens (Ø16 cm, H32 cm) for most characterizations: compression and splitting tests, and on prismatic specimens (7×7×28 cm^3) for flexural strength. After wet curing at room temperature of the laboratory (22±2°C) for 7, 14, and 28 days, the samples underwent a series of physical and mechanical tests. The results showed that workability decreased gradually as fiber content increased. Apparent density, water-accessible porosity, and capillary water absorption slightly increased with fiber content, reaching a maximum at 0.75%. On the other hand, the mechanical properties are improved: the compressive strength, splitting tensile strength, and dynamic modulus of elasticity increase significantly, with optimal gains of 15%, 18%, and 12%, respectively, compared to the control concrete. The addition of fibers also reinforced the concrete, as shown by the stress-strain curves. Those for fiber-reinforced concrete showed a slight improvement in the flexural tensile strength and displacement to failure, and a post-peak stabilization phase highlighted by the higher residual strength with fibers, unlike the control concrete, which showed brittle failure without a stabilization phase. Considering these results, annealed fiber scraps can be used as reinforcements in ordinary concrete, particularly for structural elements subject to bending, such as floors, beams, and slabs.

Keywords: Annealed Fiber; Ordinary Concrete; Physical and Mechanical Properties; Ductility

1. Introduction

For several years, the building and public works sector has undergone a dynamic evolution marked by an increased focus on mechanical performance, durability, and more environmentally friendly solutions. In this context, concrete remains the most widely used building material in the world, with an annual production exceeding ten billion tons (Miller and Moore 2020). Its success can be explained by the exceptional compromise between high mechanical

* Corresponding author: Philbert NSHIMIYIMANA

performance, high durability, and relative ease of implementation. However, despite these qualities, concrete has intrinsic weaknesses related to its porous microstructure and low tensile strength, which make it particularly vulnerable to cracking and brittle failure (Ahmad et al. 2024; Zhou et al. 2025). These limitations historically justify the use of reinforced concrete, which combines the compressive strength of the cementitious matrix of the concrete with the ability of steel reinforcement to absorb tensile constraints. The reinforcement stage, which is fundamental to the implementation of reinforced concrete, involves the use of annealed iron wires to tie the reinforcement. During this operation, iron fiber scraps were systematically generated. This situation, which is frequently observed at construction sites, is the subject of ongoing debate among practitioners. Some argue that they could contribute to strengthening the cement matrix, whereas others point to the risks of disrupting the homogeneity and durability of the material. This empirical debate is part of the broader scientific context. Numerous recent studies have focused on the incorporation of metal fibers, whether industrial or recycled, to improve the mechanical performance of concrete. Studies have confirmed that adding metal fibers can increase toughness, limit crack propagation, improve tensile strength, and increase the energy absorption capacity (Gomaa et al. 2025; Khan et al. 2022). However, these improvements depend on crucial parameters such as the fiber geometry, form factor, incorporation content, and distribution within the matrix (Zhang 2025).

Furthermore, the recovery of metal waste is now a major focus of circular economic strategies applied to the construction sector. Several recent studies have examined the use of irregular metal waste, such as steel chips, machining residues, and recycled fibers from tires, as economical and environmentally friendly substitutes for industrial metal fibers (Amran 2025; Jeron and Jose 2025; Nassiri et al. 2025). These studies show that despite their less controlled geometry, these wastes can improve the post-cracking strength, ductility, and energy absorption capacity of concrete. However, they also pointed out that their incorporation can reduce the workability and increase the porosity or capillary absorption of concrete (Aljuaydi et al. 2024; Nan et al. 2025). Approaches based on the circular economy play a key role in this move toward more sustainable materials. They encourage the recovery and reuse of waste to reduce the environmental impact on the construction industry (Peralta Ring et al. 2024). However, despite the abundance of studies on recycled metal fibers, a significant gap remains. To the best of the knowledge of the authors, few recent studies have specifically focused on the effect of annealed fiber scraps, chipped from the attachment of steel reinforcement, even though these residues constitute an abundant, locally available waste product that may be of comparable mechanical interest to short metal fibers (Abbass, Khan, and Mourad 2018).

This study aims to scientifically and quantitatively analyze the influence of incorporating annealed fiber scraps on the physical and mechanical properties of ordinary concrete. The specific objectives were to evaluate their impact on the physical properties (workability, density, porosity, and capillary absorption) and mechanical properties (compressive strength, tensile strength, and dynamic modulus of elasticity). Thus, this research aims to fill a gap in the literature while exploring a potential solution for the recovery of construction waste from the perspective of sustainability and optimization of cementitious materials.

2. Materials and methods

2.1. Materials

2.1.1. Aggregates

The sand used in this study (Figure 1a) was a natural material with a grain size of 0/5 mm, extracted from a quarry located 17 km from Bobo-Dioulasso in Burkina Faso (11.16270°N, 4.19926°W). Its main physical characteristics are listed in Table 1, and the particle size distribution curve is shown in Figure 2. The sand equivalent value of 80% indicates a low content of fine particles and confirms that it is suitable for use in concrete design. The fineness modulus (FM) of sand was 3.02, and its uniformity coefficient (UC) was 5.9. This shows a wide particle size distribution and good quality for the concrete formulation.

Two types of crushed granite gravel with particle sizes of 5/15 and 15/25 mm (Figure 1 b, c) were used. They were obtained by crushing granite extracted from a quarry located in Koro (11.14892° N, 4.18648° W), approximately 19 km from Bobo-Dioulasso, Burkina Faso. Their physical and mechanical characteristics are presented in Table 1, and their respective particle size distribution curves are shown in Figure 2. The Los Angeles test values were 24% for 5/15 mm gravel and 26% for 15/25 mm gravel, both below the 30% threshold, indicating good resistance to fragmentation. Furthermore, surface cleanliness measurements, with results of 2% and 1%, confirmed that these materials were clean. All these mechanical and physical properties validate their use in concrete formulations.

Figure 1 Aggregates used for the study: sand (a), 5/15 gravel (b), and 15/25 gravel (c)

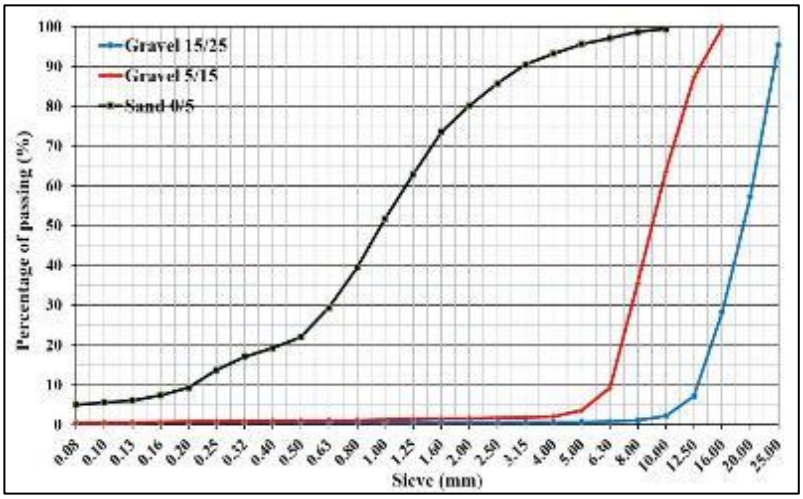

Figure 2 Particle size distribution of aggregates

Table 1 Physical and mechanical characteristics of aggregates

Designation	**Natural sand 0/5**	**Crushed granite gravel 5/15**	**Crushed granite gravel 15/25**
Apparent density NF (EN1097-3 2018)	1.76 ± 0.01	1.43 ±0.05	1.47 ± 0 .04
Absolute density (EN1097-7 2008)	2.63 ± 0.05	2.73 ±0.02	2.72 ± 0,05
Los Angeles (%) (EN1097-2 2010)	-	23.6 ± 0.5	26.4 ± 0.5
Surface cleanliness (%) (P18-591 1990)	-	2 ± 0.5	1± 0.7
Sand equivalent (%) (AFNOR NF EN 933-9 2022)	80 ± 2.5	-	-

2.1.2. Binder and metal fibers

Portland cement type CEM II 42.5 R, with an average compressive strength of 40 MPa and produced in Burkina Faso by CIMASSO, was used in the concrete mix design.

The fibers were scraps of the annealed fiber chipped from the attachment of reinforced concrete structures (**Figure 3**a). The use of these fiber scraps in reinforced concrete construction sites is a subject of debate. It is in this context that the present study assesses the impact of incorporating them into concrete, both in its fresh and hardened states. The fiber scraps were collected from the reinforcement stations and cut to a uniform length of 30 mm (**Figure 3**b). Their diameter (Ø) was 1 mm, and their specific weight was 7.97 kg/l.

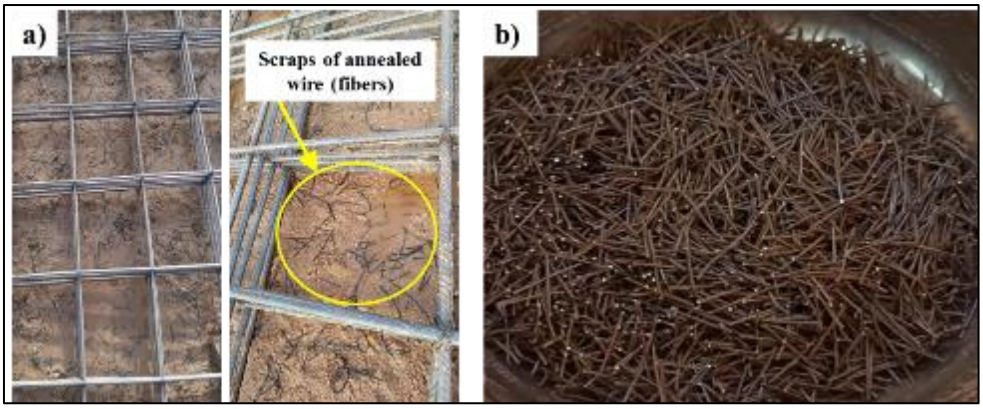

Figure 3 The annealed fiber: scraps scattered around the construction site (a) and cut to 3 cm lengths (b)

2.2. Experimental Methods

2.2.1. Design and curing conditions of concrete specimens

To highlight the influence of the fiber content (annealed fiber scraps) in concrete, four types of composites were designed based on the work of Grünewald (Grunewald 2007). This indicates that fiber-reinforced concrete generally contains approximately 1% fiber-by-volume. In the present study, the metal fiber incorporation rates selected were 0, 0.25, 0.5, and 0.75% of the concrete volume. The proportions of the base materials (sand, gravel, cement, and water) for the reference concrete mix (without fibers) were determined using the classic Dreux-Gorisse method (Hamza et al. 2020). The desired strength at 28 days was set at 25MPa with a slump of 7 ± 1 cm for plastic consistency. For the other three composites, the metal fiber content was adjusted according to the volume of the concrete. **Table 2** presents the designation of the composites as well as the masses of the different base materials used to design one cubic meter of concrete for each composite.

Concrete was prepared in two stages. The first stage consisted of homogenizing the dry materials, including the fibers, using a concrete mixer for 3 min. Subsequently, the required amount of water was added gradually. The concrete mixer was then operated for another 5 min to obtain homogeneous flesh concrete. This was used to fill the experimental molds in two layers, each of which was vibrated using a vibrating needle to ensure that the concrete was compacted and eliminate air bubbles. Two types of test specimens were used in this study. Cylindrical test specimens (Ø16 × H32 cm) were used for all characterization tests, except for the flexural strength test. Prismatic test specimens (7 × 7 × 28 cm^3) were used for the flexural strength test. Twenty-four hours after the concrete was placed in the molds, the test specimens were removed from the molds and stored in a water tank maintained at a temperature of 22 ± 5 °C until the scheduled test dates: 7, 14, and 28 days. The test specimens for characterization are shown in **Figure 4**

Table 2 Masses of the different materials used to design 1 m^3 of concrete of the different composites

	Mix designs			
Materials	CF0	CF0.25	CF0.50	CF0.75
Cement (Kg)	380	380	380	380
Water (Kg)	199	199	199	199
Sand (Kg)	696	696	696	696
Gravels 5/15 (Kg)	148	148	148	148
Gravels 15/25 (Kg)	977	977	977	977
water/cement (W/C)	0.52	0.52	0.52	0.52
Fibers (Kg)	-	19.9	39.8	59.7

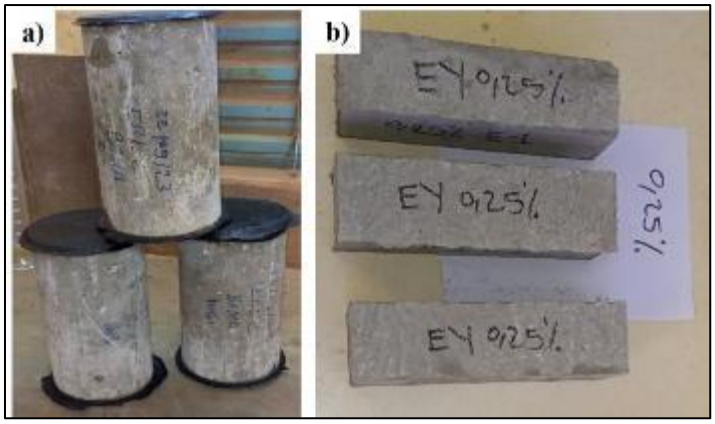

Figure 4 *C*ylindrical (a) and prismatic (b) concrete samples

2.2.2. Characterization of Physical Properties

The fresh concrete's workability was tested in accordance with NF EN 1015-3 (NF EN 12350 - 2 2019). The bulk density, (ρ_{app}), and water-accessible porosity (P) of the hardened samples were obtained using equation 1 and 2, where Mair is the mass of the saturated sample weighed in air (g), m_{water} is the mass of the saturated sample weighed in water (g), m_{dry} is the mass of the dry sample (g), and ρ_{water} is the density of water (g/cm^3). The water capillary absorption was determined using the square root of time according to equation 3. The bottom surfaces of the samples were partially immersed in water at a depth of 1 ± 0.5 cm. The wet masses were measured at intervals corresponding to t = 0.17, 0.5, 1, 2, 4, 8, 16, and 24 h of capillary immersion. The capillary absorption coefficient was calculated using equation 3. CW is the water capillary absorption (g/cm^2.min^{½}), M_{Wt} is the wet mass measured at time t (g), Mdry is the constant dry mass of the sample (g), and S is the sample's cross-section area (cm^2).

$$\rho_b = M_d \times \rho_{w_t} / \left(M_{Sat}air - M_{SatW_t}\right) \quad (1)$$

$$P = \left(M_{Sat}air - M_{dry}\right) / \left(M_{Sat}air - M_{SatW_t}\right) \quad (2)$$

$$CW = 100 \times \left(M_{W10} - M_{dry}\right)/S \times \sqrt{10} \quad (3)$$

2.2.3. Characterization of mechanical Properties

The tests of compressive strength were performed on three cylindrical specimens of each mix design using a CONTROLAB hydroelectric press with a capacity of 2 000 kN. The specimens were subjected to an increasing load at a rate of 0.25 kN/s until failure. The compressive strength, RC (MPa), is the ratio of the load at failure, P (N), to the cross-sectional area, S (mm^2), of the specimen (Equation 4).

The splitting tensile strength was determined using a splitting tensile test. It involves measuring the load, P (N), necessary to break a cylindrical specimen subjected to linear diametral compression. The splitting tensile strength, R_S (MPa), was calculated using Equation (5), where R (mm) is the radius and H (mm) is the height of the sample.

Flexural tensile strength was measured using a Controlab hydraulic press equipped with a three-point bending device. It was determined using equation (6). R_f is the three-point flexural strength (MPa); F_l is the bending force (kN); L is the length of the test piece (cm); B is the base of the test piece (cm); and H is the height of the test piece (cm).

The Pundit is a nondestructive test that evaluates the quality of concrete by measuring the speed at which ultrasonic waves travel through it. The device, shown in the **Figure 5**, includes an ultrasonic transmitter and receiver. To ensure optimal contact between them and the test piece, the cylindrical surfaces of the test piece must be flat and smooth. Once the device was turned on, the wave velocity was displayed directly. This is then combined with other parameters, such as the density and Poisson's ratio, to determine the dynamic modulus of elasticity Ed (Pa) using equation (07). V is the ultrasonic velocity (m/s), ν is Poisson's ratio (0.15), and ρ is the density of the concrete (kg/m^3).

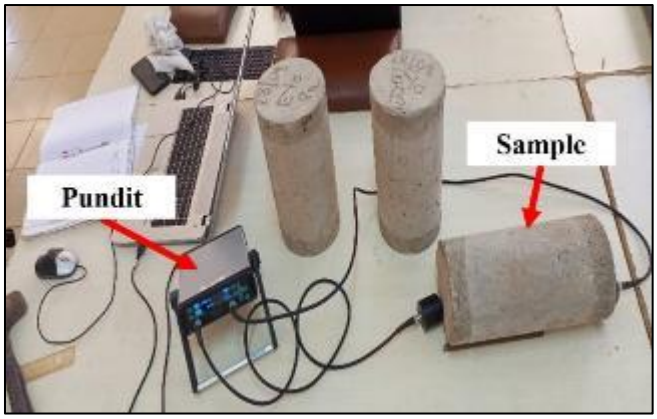

Figure 5 Ultrasonic velocity measuring device

$$R_C = P/S \quad (4)$$

$$R_S = P/\pi RH \quad (5)$$

$$R_F = 3FlL/2bH^2 \quad (6)$$

$$Ed = V^2\rho\,(1+\nu) \times (1-2\nu)/(1-V) \quad (7)$$

3. Results and discussions

3.1. Physical properties

3.1.1. Workability of flesh concrete

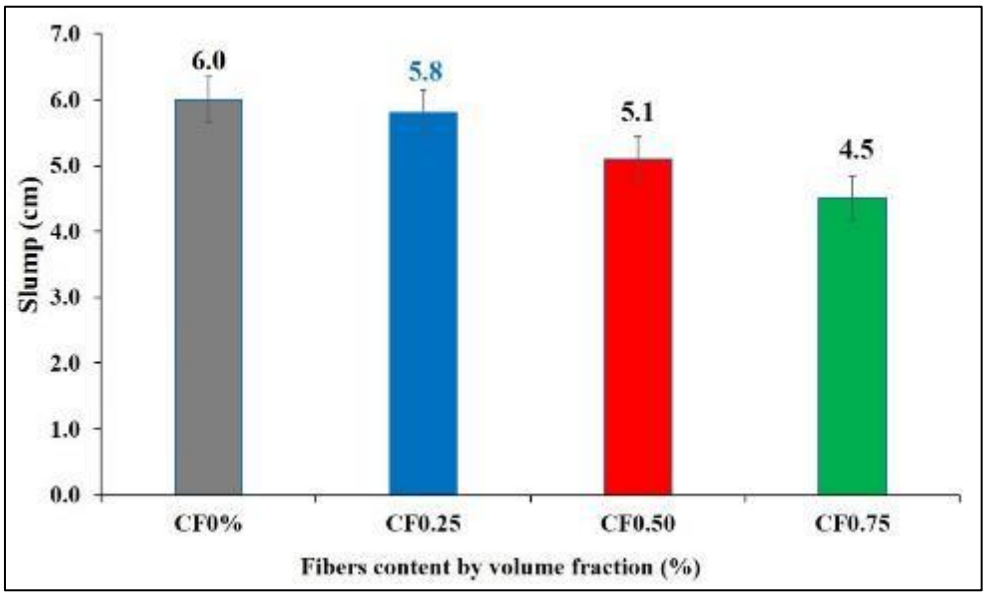

Figure 6 Workability of concrete depending on fiber content

Figure 6 illustrates the evolution of concrete workability as a function of fiber content, evaluated using the slump test. The measured values were 6, 5.8, 5.1, and 4.5 cm for fiber contents of 0, 0.25, 0.50, and 0.75%, respectively. These results show a slight decrease in workability with increasing fiber content, indicating that fiber-reinforced concrete is less workable than fiber-free concrete. This reduction is mainly due to the increase in concrete viscosity caused by the incorporation of fibers, which however maintain similar plastic class (5-7 cm of slump) except with 0.75%. Similar observations have been reported previously. For example, Uygunoglu (Uygunog 2011) observed a decrease in

workability with the addition of 3 cm and 6 cm steel fibers, while emphasizing the influence of fiber geometry and shape on this behavior. This phenomenon is attributed to the fact that the fibers increase the friction with the cement matrix. Furthermore, owing to their high specific surface area, fibers require a greater amount of water to be properly coated, which reduces the amount of water available for complete cement hydration (Katkhuda and Shatarat 2017).

3.1.2. Apparent density and porosity of hardened concrete

Figure 7 shows the apparent densities of the concrete cured for 28 days. The results indicate that the addition of fibers has only a limited effect on the apparent density of the test specimens. Indeed, the density of concrete without fibers is 2.31, while that of concrete containing fibers (0.25; 0.5, and 0.75%) is 2.33, 2.34, and 2.35 g/cm^3, respectively. This slight increase can be explained by the high density of steel fibers compared to that of other concrete constituents, such as aggregates and cement. These observations are consistent with the work of Ali et al. (Ali et al. 2011), who also reported a moderate increase in the apparent density of the concrete from 1.76 to 1.87 g/cm^3, depending on the fiber content (0 to 1%).

Furthermore, **Figure 8** illustrates the evolution of the water-accessible porosity as a function of the fiber content. The porosity also slightly increased from 8.8% for fiber-free concrete to 9.93% for a fiber content of 0.75%, which corresponds to an optimal relative increase of 13% between the reference concrete and 0.75% fiber-reinforced concrete. This increase could be attributed to the stiffness of the fibers, which limits effective densification during concrete vibration, thus leading to the formation of microcavities in the cement matrix. In addition, a higher fiber content promotes random meshing, creating more pores and increasing the porosity. These results are consistent with those of Simões et al. (T. Simões, H. Costa, D. Dias-da-Costa, Júlio 2017), who observed a similar increase in porosity in polypropylene fiber-reinforced concrete, which they attributed to the presence of trapped air at the interfacial transition zone between the fibers and cement matrix.

However, the change in the porosity of the fiber-reinforced concrete does not appear to be consistent with that of the bulk density. Indeed, an increase in porosity normally leads to a decrease in density. However, in the present case, the opposite phenomenon was observed due to the higher density of fiber, although the increase in the density remained very small.

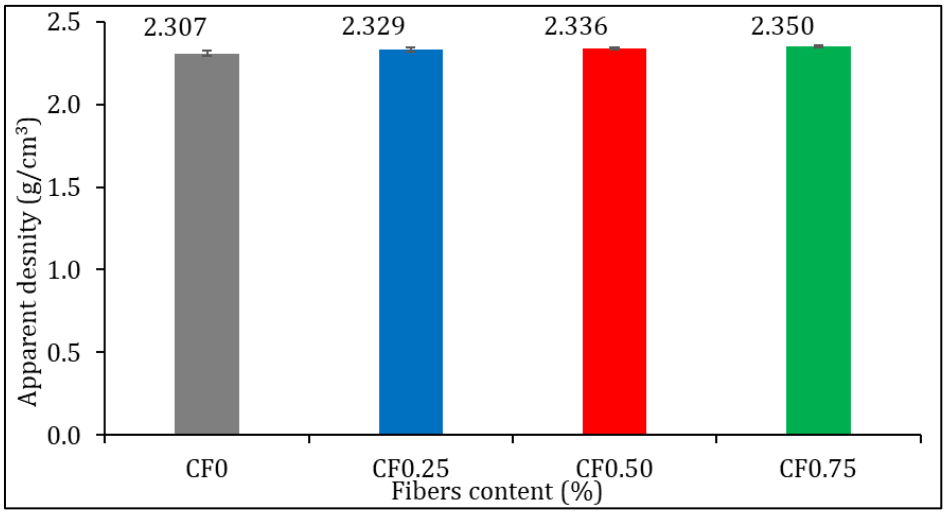

Figure 7 Apparent density of concrete depending on fiber content

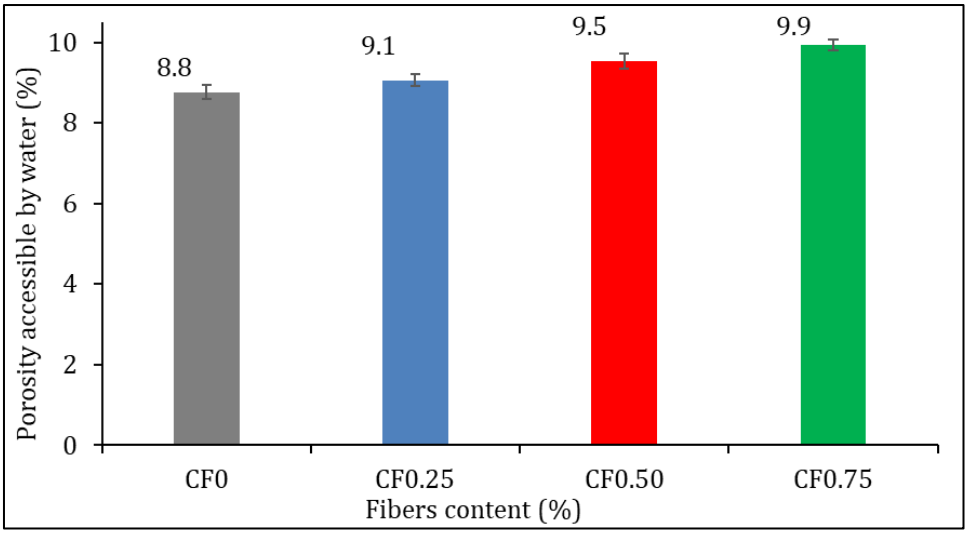

Figure 8 Porosity accessible by water of concrete depending on fiber content

3.1.3. Capillary absorption hardened concrete

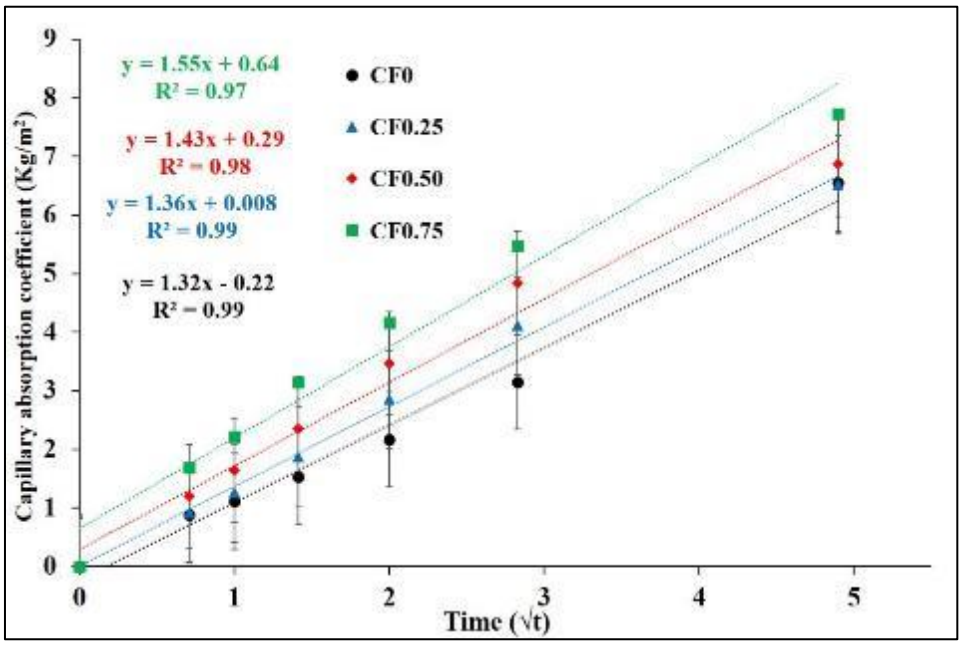

Figure 9 Evolution of water capillary absorption between 1 and 24 hours

Table 3 Correlation between capillary absorption and water-accessible porosity

Designation	Sorptivity (kg/m²h$^{1/2}$)	Porosity (%)
CF0	1.32	8.76
CF0.25	1.36	9.05
CF0.50	1.43	9.55
CF0.75	1.55	9.93

Figure 9 illustrates the evolution of capillary absorption in concrete as a function of time and fiber content. This parameter increases with the percentage of fibers; concrete with 0.75% fibers (CF0.75) has the highest absorption coefficient, which in turn exceeds that of concrete with 0.25% fibers (CF0.25). This evolution is consistent with the

results for the water-accessible porosity. A more porous matrix with a larger pore volume can absorb more water, thereby directly influencing the absorption coefficient. Therefore, porosity and capillary absorption appear to be closely linked. Table 3 shows the sorptivity and porosity of the concrete as a function of the fiber content. The sorptivity increased with increasing fiber content. The reference concrete CF0 has the lowest sorptivity of at 1.32 kg/m^2·h$^{1/2}$ while the 0.75% fiber-reinforced concrete (CF0.75) reaches the maximum value of 1.55 kg/m^2·h$^{1/2}$. This trend was consistent with the porosity measurements. The samples with the highest porosity, such as CF0.5 (9.55%) and CF0.75 (9.93%), also had the highest sorptivity of 1.43 and 1.55 kg/m^2·h$^{1/2}$, respectively, confirming that the capillary absorption rate increased with the addition of fibers, as shown in **Figure 9**. According to Ziane et al. (Ziane, Khelifa, and Mezhoud 2020), The incorporation of polypropylene fibers into concrete tends to increase its water absorption, and this increase is proportional to the length and dosage of the fibers. The authors attributed this phenomenon to the poor fiber distribution, accessible porosity, and size of the capillaries generated by these fibers.

3.2. Mechanical properties of hardened concrete

3.2.1. Compressive strength

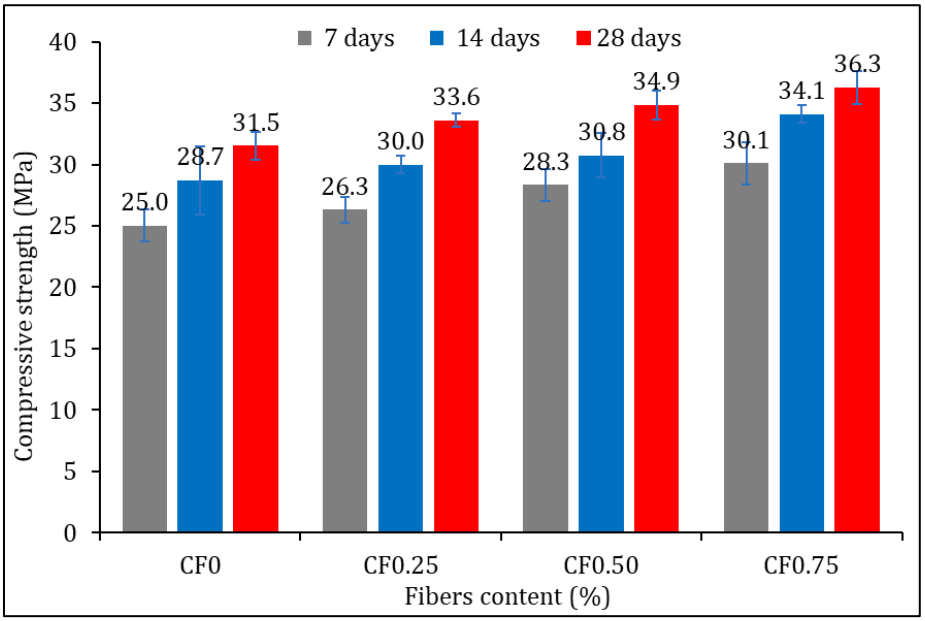

Figure 10 Evolution of compressive strength as a function of curing time and fiber content

Figure *10* illustrates the evolution of compressive strength of concrete as a function of the fiber content and curing time. An overall improvement in this mechanical parameter was observed with the incorporation of fibers at all curing ages. The maximum strengths are obtained with a fiber content of 0.75% (CF0.75), reaching 30.1 MPa at 7 days, 34.1 MPa at 14 days, and 36.2 MPa at 28 days. In comparison, fiber-free concrete (CF0) has the lowest strength, with 25 MPa, 28.7 MPa, and 31.6 MPa at the same intervals. This increase represents 20%, 19%, and 15% increases between the CF0 and CF0.75 concrete, respectively, confirming the significant beneficial effect of the fibers. The positive influence of metal fibers can be explained by their rigidity, which contributes to the confinement of the internal components of the matrix and improves the structural integrity of the concrete. In addition, the addition of fiber slows the propagation of microcracks to failure, reinforcing the overall resistance of the material to stress induced by loads. These observations are consistent with those of Karthik et al. (Karthik et al. 2024), who also observed a significant increase in compressive strength with the addition of polypropylene and steel fibers. These authors attributed this improvement to good adhesion between the binder paste and the fibers, which facilitates the transfer of stress within the material. A similar trend was reported by Song and Hwang (Song and Hwang 2004), who demonstrated an improvement in the mechanical strength of concrete with the incorporation of steel fibers in proportions of up to 2% by volume. This phenomenon is explained by the absorption of compressive loads by the fibers once the concrete matrix reaches its breaking point, which is made possible by the metallic nature of the fibers, which are more resistant than agricultural fibers.

On the other hand, the study of Islam and Gupta (Islam et al. 2020) on concrete containing 0.1% and 0.3% polypropylene fibers showed a decrease of approximately 10% in the compressive strength compared to the control concrete. This reduction was attributed to the creation of interfacial transition zones within the matrix, which reduced the strength of the material.

3.2.2. Splitting tensile strength

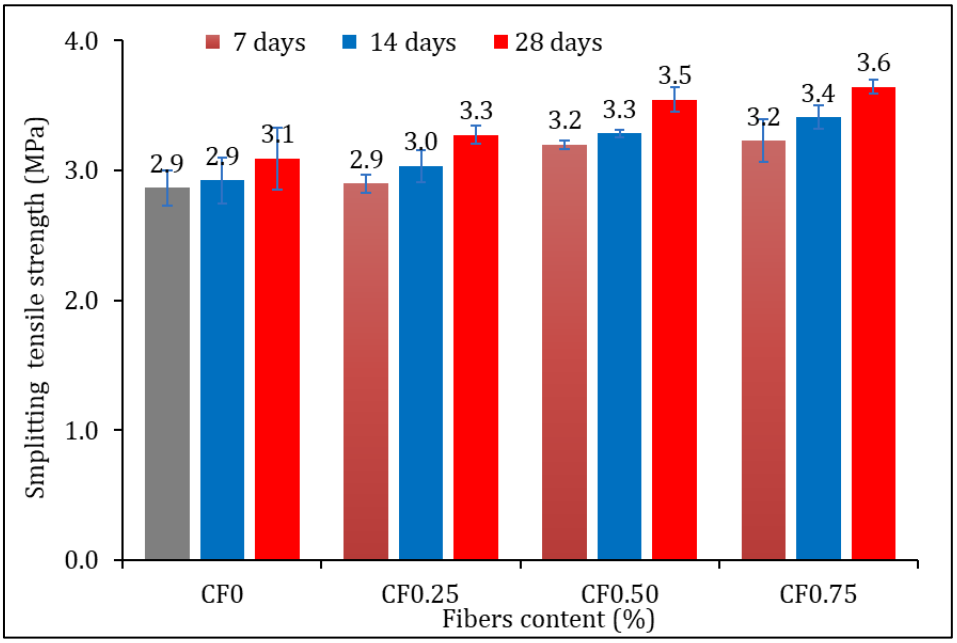

Figure 11 Evolution of splitting tensile strength as a function of curing time and fiber content

Figure 11 shows the evolution of the splitting tensile strength for different concretes as a function of the steel fiber content and curing time. This behavior is like that of the compressive strength, although with a more pronounced improvement. Composites containing annealed iron fibers thus exhibit a higher tensile strength than fiber-free concrete. For CF0.75 concrete, the optimal increase in this parameter was estimated to be 12%, 16%, and 18% after 7, 14, and 28 d of curing, respectively, compared to the CF0 control concrete. This improvement can be explained by the suture role played by the fibers in response to cracks induced under load; their presence counteracts the propagation of microcracks, prevents the formation of macrocracks, and thus strengthens the performance of concrete under tensile stress (Banthia et al. 2014). In addition, the inherently high mechanical strength of steel fibers allows them to contribute directly to the load transfer. In the absence of fibers, microcracks coalesce and orient themselves to form macrocracks, leading to composite failure. Song and Hwang (Song and Hwang 2004) also demonstrated a significant improvement in the tensile strength of concrete through the addition of steel fibers. Will et al. (Wille, Kim, and Naaman 2011) observed the same phenomenon when incorporating two types of fibers (straight and twisted) at concentrations ranging from 1.5% to 2.5% of the concrete volume. The tensile strength increased from 8 to 14 MPa for straight fibers and from 8 to 15 MPa for twisted fibers, confirming the beneficial influence of the fibers on the cement matrix.

3.2.3. Flexural tensile strength

Figure 12 shows the evolution curves of bending stresses as a function of displacement for each fiber content in different concretes. A notable increase in peak stress was observed in fiber-reinforced concrete, particularly for 0.75% content (CF0.75). The curve for the control concrete (CF0), without fibers, is characterized by two phases: an initial upward phase, which is not completely linear until failure, followed by a second sharp downward phase, marked by the appearance and propagation of the cracks which is characteristic of brittle behavior. However, fiber-reinforced concrete exhibits three distinct phases: the previous two phases and a stabilization phase after the downward phase. The ascending and descending phases were linear. This final stabilization phase is attributable to the presence of fibers, which results in less brittle behavior of the composites. After the initial cracking of the concrete, the fibers overcome the tensile stresses, thus improving the overall strength. The failure peaks of the reinforced concrete appear more rounded than those of the control concrete, which are very sharp. The more pronounced stabilization post peak for concrete with 0.75% fibers indicates greater stress transfer to fibers than control concrete. These results are consistent with the work of Wang et al. (Wang et al. 2019), who attributed the improved ductility of fiber-reinforced composites to the transfer of load after cracking to the fibers via their interfacial bonds with the matrix. This mechanism allows the fiber-reinforced concrete to exceed the load-bearing capacity of the concrete alone. Finally, Karthik et al. (Karthik et al. 2024) explained this performance gain by a crack-bridging mechanism induced by the fibers, which cover larger openings and are more resistant to detachment, thereby delaying crack propagation under bending or torsional loads.

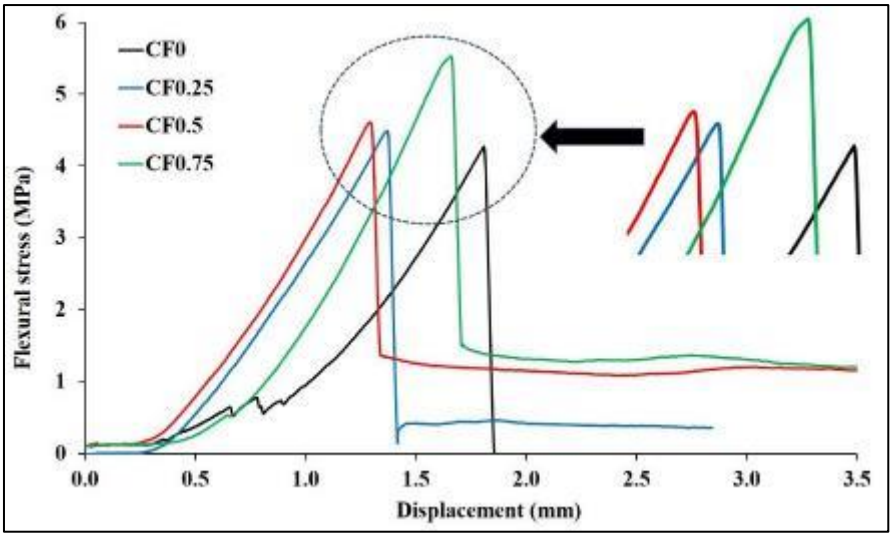

Figure 12 Evolution of flexural tensile stress in concretes as a function of displacement

3.2.4. Dynamic modulus of elasticity

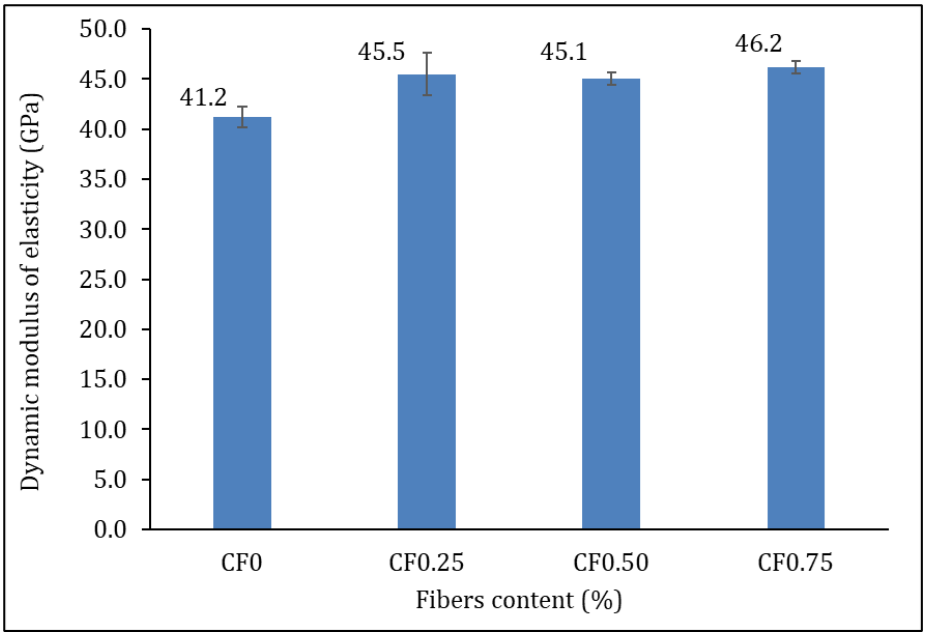

Figure 13 Dynamic modulus of elasticity of concrete composites

Figure 13 illustrates the evolution of the dynamic elasticity modulus of concrete as a function of the content of annealed steel fibers. Overall, an increase in this parameter was observed with an increase in the percentage of fibers. The minimum value of 41.2 GPa was observed for the control concrete without fibers (CF0), whereas the maximum value of 46.2 GPa was reached with a fiber content of 0.75% (CF0.75), representing a slightn increase of approximately 12% compared to the control concrete. This increase can be explained by the presence of metal fibers, which are more conductive to waves than the cement matrix, accelerating their propagation, particularly in the case of CF0.75 concrete.

These results corroborate those obtained for compressive strength (**Figure 10**), where the best performance was observed for concrete containing 0.75% fibers. They also agree with the work of Salih et al. (Salih 2012), who showed that adding steel fibers increases the elastic modulus of concrete. However, the change in the dynamic elastic modulus may vary depending on the nature of the fibers. For example, Suhaendi and Horiguchi (Suhaendi and Horiguchi 2006) studied the effects of steel and polypropylene fibers. The addition of steel fibers at concentrations of 0.25% and 0.5% increased the modulus of elasticity by 7% to 22% compared to the control concrete, while polypropylene fibers, on the contrary, reduced its value. Furthermore, the slight decrease in the modulus observed for CF0.5 concrete compared to

CF0.25 could be attributed to a lack of homogeneity in the matrix, such as an uneven fiber distribution. Despite this variation, the modulus value for CF0.5 remains higher than that of CF0 concrete, confirming the positive influence of iron fibers on the dynamic modulus of elasticity.

4. Conclusion

This study aimed to evaluate the influence of incorporating annealed fiber scraps on the properties of concrete. Characterization of fiber-reinforced concrete with contents ranging from 0% to 0.75% led to the following conclusions:

- Physical properties: The addition of fibers slightly reduced the workability of fresh concrete, with the slump on Abrams cone decreasing from 6 cm for the control concrete to 4.5 cm for concrete with 0.75% fibers. This decrease was attributed to the fibers trapping the flesh concrete, which limited the slump. In addition, the density of hardened concrete increased slightly with fiber content, reaching a maximum value of 2.35 g/cm^3 at 0.75%. However, the porosity increased with the fiber content, which significantly influenced the water absorption by capillarity. This increase can be explained by the pore creation by the fibers to direct water in the longitudinal direction.
- Mechanical properties: The addition of annealed fibers improves the overall mechanical performance. After 28 d of curing, the compressive strength and splitting tensile strength increased, with optimal gains of 15% and 18%, respectively, for a fiber content of 0.75% compared to the control concrete. These improvements are linked to the ability of the fibers to absorb stress after matrix cracks and to limit crack propagation. The flexural strengths revealed less brittleness, which was particularly pronounced for concrete containing 0.75% fibers. Thus, the fibers mitigated the brittle behavior of the material owing to their adhesion to the matrix. Finally, the dynamic modulus of elasticity also slightly increased with the fiber content, with a maximum value of 0.75%.

The results showed that the engineering properties of concrete were enhanced by incorporating annealed fiber scraps. Although this study opens promising prospects for the recovery of this fiber waste, further characterization is needed to better understand the fiber-matrix interface, particularly through microstructure observation. Durability tests, such as acid attacks, would also make it possible to evaluate the long-term behavior of fiber-reinforced concretes.

Compliance with ethical standards

Acknowledgments

The authors would like to express their sincere thanks to the management of the LNBTP and Institut 2iE, who allowed some of these studies to be carried out within their institutions.

Disclosure of conflict of interest

No conflict of interest to be disclosed.

References

[1] Abbass, Wasim, M. Iqbal Khan, and Shehab Mourad. 2018. "Evaluation of Mechanical Properties of Steel Fiber Reinforced Concrete with Different Strengths of Concrete." *Construction and Building Materials* 168:556–69.

[2] AFNOR NF EN 933-9. 2022. *Essais Pour Déterminer Les Caractéristiques Géométriques Des Granulats - Partie 9 : Qualification Des Fines - Essais Au Bleu de Méthylène*.

[3] Ahmad, Jawad, Yasir Mohammed Jebur, Muhammad Tayyab Naqash, Muhammad Sheraz, Ahmed Hakamy, and Ahmed Farouk Deifalla. 2024. "Improvement in the Strength of Concrete Reinforced with Agriculture Fibers : Assessment on Mechanical Properties and Microstructure Analysis." *Engineered Fibers and Fabrics* 19. doi: 10.1177/15589250241226480.

[4] Ali, Nicolas, Mohammad Shekarchi, Mehrdad Mahoutian, and Parviz Soroushian. 2011. "Mechanical Properties of Hybrid Fiber Reinforced Lightweight Aggregate Concrete Made with Natural Pumice." 25:2458–64. doi: 10.1016/j.conbuildmat.2010.11.058.

[5] Aljuaydi, Fahad, Rajab Abousnina, Omar Alajarmeh, and Abdalrahman Alajmi. 2024. "The Influence of Fibres on the Properties and Sustainability of Oil-Impacted Concrete." *Sustainability* 16(17):7344.

[6] Amran, Mugahed. 2025. "Innovative Technology for Converting Automobile Tire Waste Bead Wires into Recycled Steel Fibers for Sustainable Concrete Composites: Insights for the Al-Kharj Governorate Construction Industry." *International Journal of Building Pathology and Adaptation* 43(4):665–92.

[7] Banthia, Nemkumar, Fariborz Majdzadeh, Jane Wu, and V. Bindiganavile. 2014. "Fiber Synergy in Hybrid Fiber Reinforced Concrete (HyFRC) in Flexure and Direct Shear." *Cement and Concrete Composites* 48:91–97.

[8] EN1097-2, NF. 2010. *Essais Pour Déterminer Les Caractéristiques Mécaniques et Physiques de Granulats. Méthodes Pour La Détermination de La Résistance à La Fragmentation*.

[9] EN1097-3. 2018. *Détermination de La Masse Volumique En Vrac*.

[10] EN1097-7, NF. 2008. *Détermination de La Masse Volumique Absolue Du Filler - Méthode Au Pycnomètre*.

[11] Gomaa, Ahmed M., Kamal Hafez, Bishoy Refaat, Hashem Ahmed, Mina Hesham, Mohamed Ehab, Raafat Osama, Moaz Walid, and Khaled Samy. 2025. "Analyzing the Mechanical Properties of Fiber-Reinforced Concrete : A Bibliometric Review of Current Trends , Research Advances , and Future Outlook." *Advanced Sciences and Technology Journal* 2(3):1–18.

[12] Grunewald, Steffen. 2007. "Performance-Based Design of Self-Compacting Fibre Reinforced Concrete." *Structural Concrete* (3):156–61.

[13] Hamza, Chbani, Saadouki Bouchra, Boudlal Mostapha, and Barakat Mohamed. 2020. "Formulation of Ordinary Concrete Using the Dreux-Gorisse Method." *Procedia Structural Integrity* 28:430–39.

[14] Islam, Mohammad Shariful, Tausif E. Elahi, Azmayeen Rafat Shahriar, and Nashid Mumtaz. 2020. "Effectiveness of Fly Ash and Cement for Compressed Stabilized Earth Block Construction." *Construction and Building Materials* 255:119392.

[15] Jeron, R., and Y. Stalin Jose. 2025. "Investigating Porosity and Strength Characteristics of Novel Concrete Design Based on Recycled Ceramics, Steel Fiber, and Industrial Chip Wastes Using Novel Deep Learning." *Journal of Building Engineering* 113123.

[16] Karthik, S., K. Saravana Raja, G. Murali, Sallal R. Abid, and Saurav Dixit. 2024. "Impact of Various Fibers on Mode I , III and I / III Fracture Toughness in Slag , Fly Ash , and Silica Fume-Based Geopolymer Concrete Using Edge-Notched Disc Bend Specimen." *Theoretical and Applied Fracture Mechanics* 134:1–20.

[17] Katkhuda, Hasan, and Nasim Shatarat. 2017. "Improving the Mechanical Properties of Recycled Concrete Aggregate Using Chopped Basalt Fibers and Acid Treatment." *Construction and Building Materials* 140:328–35. doi: 10.1016/j.conbuildmat.2017.02.128.

[18] Khan, Inayat Ullah, Akhtar Gul, Khalid Khan, and Saeed Akbar. 2022. "Mechanical Properties of Steel-Fiber-Reinforced Concrete †." *Engineering Proceedings* 22(6):1–7.

[19] Miller, Sabbie A., and Frances C. Moore. 2020. "Climate and Health Damages from Global Concrete Production." *Nature Climate Change* 10(5):439–43.

[20] Nan, Fang, Qing Shen, Shuang Zou, Haijing Yang, Zhenping Sun, and Jingbin Yang. 2025. "Capillary Water Absorption Characteristics of Steel Fiber-Reinforced Concrete." *Buildings* 15(9):1542.

[21] Nassiri, Somayeh, Souvik Roy, Md Mostofa Haider, Ali A. Butt, Gandhar A. Pandit, and John T. Harvey. 2025. "Literature Review and Industry Survey of Recycled Fibers from Novel and Existing Source Materials for Concrete Use."

[22] NF EN 12350 - 2. 2019. "12350-2 Juin (2019) Essais Pour Béton Frais-Partie 2: Essai d'affaissement." *NF EN* 12390–93.

[23] P18-591, NF. 1990. *Granulats - Détermination de La Propreté Superficielle*.

[24] Peralta Ring, Rocio, Gisela Cordoba, Natalia Delbianco, Carla Priano, and Viviana Rahhal. 2024. "Circular Economy Approach: Recycling Toner Waste in Cement-Based Construction Materials." *Sustainability* 16(11):4707.

[25] Salih, Shakir A. 2012. "Improving the Modulus of Elasticity of High Performance Concrete by Using Steel Fibers." *Anbar Journal of Engineering Science* 5(Special-Part 1):205–16.

[26] Song, P. S., and S. Hwang. 2004. "Mechanical Properties of High-Strength Steel Fiber-Reinforced Concrete." 18:669–73. doi: 10.1016/j.conbuildmat.2004.04.027.

[27] Suhaendi, Sofren Leo, and Takashi Horiguchi. 2006. "Effect of Short Fibers on Residual Permeability and Mechanical Properties of Hybrid Fibre Reinforced High Strength Concrete after Heat Exposition." *Cement and Concrete Research* 36(9):1672–78.

[28] T. Simões, H. Costa, D. Dias-da-Costa, Júlio, E. N. B. S. 2017. "Influence of Fibres on the Mechanical Behaviour of Fibre Reinforced Concrete Matrixes." *Construction and Building Materials* 137(April):548–56. doi: 10.1016/j.conbuildmat.2017.01.104.

[29] Uygunog, Tayfun. 2011. "Effect of Fiber Type and Content on Bleeding of Steel Fiber Reinforced Concrete." 25:766–72. doi: 10.1016/j.conbuildmat.2010.07.008.

[30] Wang, Xinzhong, Jun He, Ayman S. Mosallam, Chuanxi Li, and Haohui Xin. 2019. "The Effects of Fiber Length and Volume on Material Properties and Crack Resistance of Basalt Fiber Reinforced Concrete (BFRC)." *Advances in Materials Science and Engineering* 2019(1):7520549.

[31] Wille, Kay, Dong Joo Kim, and Antoine E. Naaman. 2011. "Strain-Hardening UHP-FRC with Low Fiber Contents." *Materials and Structures* 44(3):583–98.

[32] Zhang, Xv. 2025. "Properties and Applications of Steel Fiber Reinforced Concrete." *Advances in Research on Teaching* 26(2):312–19.

[33] Zhou, Jian, Yiding Dong, Tong Qiu, Jiaojiao Lv, Peng Guo, and Xi Liu. 2025. "The Microstructure and Modification of the Interfacial Transition Zone in Lightweight Aggregate Concrete : A Review." *Buildings* 15(2789):1–19.

[34] Ziane, Sami, Mohammed-Rissel Khelifa, and Samy Mezhoud. 2020. "Effet Des Paramètres de Formulation Sur Les Caractéristiques Physico-Mécaniques Des Bétons Renforcés Des Fibres de Polypropylène." *Academic Journal of Civil Engineering* 38(1):229–32.